Vibrational and Electronic Circular Dichroism Monitoring of Copper(II) Coordination with a Chiral Ligand

TAO WU,[1] XIAO-PENG ZHANG,[1] CHENG-HUI LI,[1]* PETR BOUŘ,[2]* YI-ZHI LI[1] AND XIAO-ZENG YOU[1]*

[1]*State Key Laboratory of Coordination Chemistry, Nanjing National Laboratory of Microstructures, School of Chemistry and Chemical Engineering, Nanjing University, Nanjing, China*

[2]*Institute of Organic Chemistry and Biochemistry, Praha 6, Czech Republic*

ABSTRACT Novel copper(II) coordination compounds with chiral macrocyclic imine ligands derived from *R*-/*S*-camphor were asymmetrically synthesized and characterized with the aid of chiroptical spectroscopies. Crystal structures of both enantiomers were determined by single crystal X-ray diffraction analysis. Circular dichroism (CD) spectra were analyzed using a simplified exciton model as well as quantum chemical computations. The absolute configuration of the copper (II) coordination compounds determined from CD was found consistent with the crystal data. The copper(II) complexes were further investigated by vibrational CD (VCD) measurement combined with density functional theory calculation. The complex formation was evidenced by spectral shifts of the characteristic bands in the CD and VCD spectra. *Chirality 24:451–458, 2012.* © 2012 Wiley Periodicals, Inc.

KEY WORDS: circular dichroism; vibrational circular dichroism; chiral coordination compounds; coordination process; density functional theory calculations

INTRODUCTION

Chiroptical techniques based on the different interaction of chiral molecules with left and right circularly polarized light, such as optical rotatory dispersion, Raman optical activity, circularly polarized luminescence, and circular dichroism (CD), can be conveniently used to monitor the structure of both organic and inorganic compounds. In particular, the CD spectroscopy,[1] which arises from the difference in absorption of left and right circularly polarized light, has become popular for regular chemical analysis. Commercial CD instruments are available for both the electronic CD (or just CD) and the vibrational CD (VCD): the former explores the ultraviolet–visible (UV–vis) region comprising electronic transitions, whereas the latter operates in the infrared (IR) region (especially in the mid-infrared region) and sees vibrational transitions.[2] CD spectroscopy is used as a powerful tool in stereochemical analysis for chiral organic molecules, supramolecular systems, and coordination complexes.[3–12]

The chirality of metal coordination compounds attracted chemists' attention because of its role in asymmetric catalysis, chiral recognition, optically active molecular materials, and life sciences.[13–15] VCD spectra of transition metal compounds exhibit some particular properties. For example, Nafie *et al.* discussed the role of low-lying excited electronic states in the enhancement of VCD in transition-metal coordination compounds.[16,17] Sato *et al.* emphasized the effect of d electron configurations of central transition-metal ions of tris (β-diketonato) coordination compounds on the VCD.[18,19]

Nevertheless, detailed comparisons of the CD and VCD spectra of metal complex with free ligand and theory are rather rare. In a previous study, we designed and asymmetrically synthesized a novel chiral macrocyclic imine ligands derived from *R*-/*S*-camphor and their nickel(II) coordination compounds;[20] however, the poor solubility of the nickel(II) coordination compounds inhibited the VCD measurement in solution. Moreover, it is generally believed that VCD for open-shell systems is less predictable than that of closed-shell systems, at least within the density functional theory (DFT) framework.[21,22] Therefore, the paramagnetic copper(II) coordination model compounds (Scheme 1) were asymmetrically synthesized and characterized instead. The copper(II) coordination compounds are well soluble in deuterated chloroform, which facilitated detailed VCD exploration in both mid-infrared region and C-H stretching region. The absolute configuration of both enantiomers was determined by single crystal X-ray crystallography and confirmed by electronic CD and VCD. Comparison of the spectra of metal coordination compounds with those of the free ligands indicated complex formation. The results thus show that the chiral spectroscopic techniques can be conveniently used to monitor the coordination process.

EXPERIMENTAL

General Procedures

Elemental analyses for C, H, N, and S were performed on a Perkin-Elmer 240C analyzer (Norwalk, Connecticut, USA). Electrospray ionization mass spectra (ESIMS) were recorded on a Finnigan MATSSQ 710 mass spectrometer in the range of 120–1000 amu. ^{1}H-NMR spectra were obtained on a DRX 500 NMR spectrometer. Chemical shifts are referenced to TMS. Spin–spin coupling constants are given in hertzs. Electronic absorption spectra were measured on UV-3600 spectrophotometer. CD spectra were recorded on a Jasco J-810 spectropolarimeter. IR and VCD spectra in the region of 1800–800 cm^{-1} were recorded on an IFS-66/S Fourier transform

Additional Supporting Information may be found in the online version of this article.

Contract grant sponsor: National Natural Science Foundation of China; Contract grant numbers: 91022031.21021062.21001063.
Contract grant sponsor: China Ministry of Science and Technology; Contract grant numbers: 2007CB925100.2011CB808704.
Contract grant sponsor: Grant Agency of the Czech Republic; Contract grant number: P208/11/0105.

*Correspondence to: Cheng-Hui Li and Xiao-Zeng You, State Key Laboratory of Coordination Chemistry, Nanjing National Laboratory of Microstructures, School of Chemistry and Chemical Engineering, Nanjing University, 210093 Nanjing, China. E-mail: youxz@nju.edu.cn; Petr Bouř Institute of Organic Chemistry and Biochemistry Praha 6, Czech Republic. E-mail: bour@uochb.cas.cz

DOI: 10.1002/chir.22010
Published online 28 April 2012 in Wiley Online Library (wileyonlinelibrary.com).

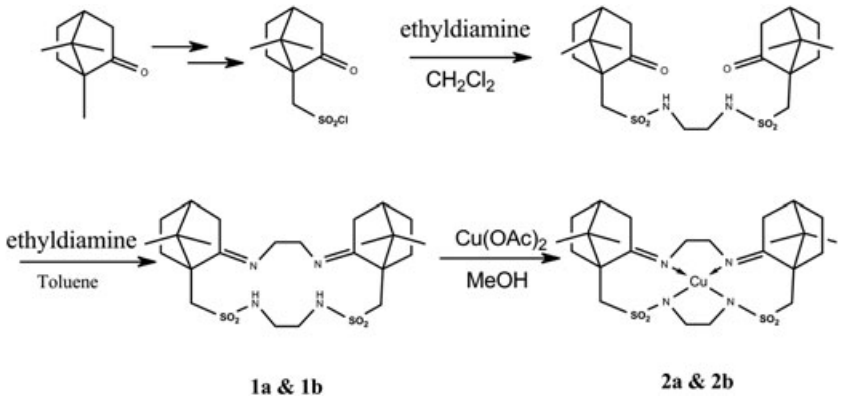

Scheme 1. Asymmetric synthesis of chiral macrocyclic imines copper(II) coordination compounds **2** (**a** derived from *R*-camphor, **b** derived from *S*-camphor).

IR spectrometer equipped with a PMA 37 VCD/IRRAS module (Bruker, Germany) using standard procedures.[6,9] The photo elastic modulator (PEM) was set to 1600 cm^{-1}, the spectral resolution was 4 cm^{-1}, and the zero filling factor was 4. A demountable cuvette A145 with KBr windows with 0.10 mm Teflon spacer was used. IR and VCD spectra in the region of 4000–2000 cm^{-1} were investigated with a Tensor 27 Fourier transform IR spectrometer equipped with a PMA 50 VCD/IRRAS module (Bruker, Germany) using standard procedures.[6,9] The PEM was set to 3000 cm^{-1}, the spectral resolution was 8 cm^{-1}, and the zero filling factor was 2. A demountable cuvette A145 with infrasil windows with 0.10 mm Teflon spacer was used. All solution samples were dissolved in deuterated chloroform to the same concentration of 0.174 mol l^{-1}. All VCD measurements were collected for 4 h composed of 12 blocks in 20 min. Baseline correction was performed with the spectra of $CDCl_3$ using the same measurement setup as for VCD. Chiral marcocyclic imines were prepared from camphor following procedures reported previously.[20] Synthesis of both copper coordination compounds enantiomers were performed under the same condition.

Synthesis of Coordination Compounds Enantiomers

130 mg (0.25 mmol) chiral macrocyclic ligand **1a** and 54 mg (0.27 mmol) copper acetate was suspended in 100 ml methanol. The mixture solution was refluxed for 0.5 h. The solvent was evaporated in vacuo. The blue residue was extracted with dichloromethane and diluted with 95% ethanol. The organic solution was carefully evaporated. After 2 days blue crystals of **2a** suitable for X-ray crystallography study were collected (95 mg, 64%). $C_{24}H_{40}N_4O_5S_2Cu$ (sample dried *in vacuo* for 12 h, -H_2O, 574.26), calcd (found): C, 50.20 (50.22); H, 6.67 (6.70); N, 9.76 (9.80); S, 11.14 (11.11). *m/z* (ESIMS): 574.17 (M^+, 73%); 596.17 ($M^+ + Na^+ - 1$, 100%); 598.18 ($M^+ + Na^+ + 1$, 52%). ^1H NMR ($CDCl_3$, 500 Hz): 0.91 (s, 3H); 0.96 (s, 3H); 1.31–1.37 (m, 1H); 1.81–1.96 (m, 2H); 1.97–2.04 (m, 2H); 2.17, 2.19 (d, 1H); 2.40, 2.43 (d, 1H); 3.01, 3.47 (AB, J = 14.4, 2H); 3.35–3.41 (m, 2H); 3.44 (s, 2H); 8.21 (s, 1H). Coordination compound **2b** was obtained with the same procedure from **1b**, blue crystals, $C_{24}H_{40}N_4O_5S_2Cu$ (sample dried *in vacuo* for 12 h, -H_2O, 574.26), calcd (found): C, 50.20 (50.21); H, 6.67 (6.69); N, 9.76 (9.81); S, 11.14 (11.12). *m/z* (ESIMS): 574.17(M^+, 73%); 596.17($M^+ + Na^+ - 1$, 100%); 598.18($M^+ + Na^+ + 1$, 52%). ^1H NMR ($CDCl_3$, 500 Hz): 0.91(s, 3H); 0.96 (s, 3H); 1.31–1.37 (m, 1H); 1.81–1.96 (m, 2H); 1.97–2.04 (m, 2H); 2.17, 2.19 (d, 1H); 2.40, 2.43 (d, 1H); 3.01, 3.47 (AB, J = 14.4, 2H); 3.35–3.41 (m, 2H); 3.44 (s, 2H); 8.21(s, 1H).

X-Ray Crystallography

Single crystal X-ray diffraction measurements for coordination compounds **2a** and **2b** were carried out on a Bruker SMART APEX CCD on the basis of diffractometer operating at room temperature. Intensities were collected with graphite monochromatized Mo Kα radiation (λ = 0.71073 Å) operating at 50 kV and 30 mA, using $\omega/2\theta$ scan mode. The data reduction was made with the Bruker SAINT package.[23] Absorption corrections were performed using the SADABS program.[24] The structures were solved by direct methods and refined on F^2 by full-matrix least-squares using SHELXL-97 with anisotropic displacement parameters for all nonhydrogen atoms in all two structures. Hydrogen atoms bonded to the carbon atoms were placed in calculated positions and refined as riding mode, with C-H = 0.93 Å (methane) or 0.96 Å (methyl) and U_{iso} (H) = 1.2U_{eq} ($C_{methane}$) or U_{iso} (H) = 1.5U_{eq} (C_{methyl}). The water hydrogen atoms were located in the difference Fourier maps and refined with an O-H distance restraint [0.85(1) Å] and U_{iso} (H) = 1.5U_{eq} (O). All computations were carried out using the SHELXTL-97 program package.[25] CCDC 819554 (**2a**) and 819555 (**2b**) contain the supplementary crystallographic data for this paper. These data can be obtained free of charge from the Cambridge Crystallographic Data Centre via www.ccdc.cam.ac.uk/data_request/cif.

Computational Section

The calculations were carried out with Gaussian09 programs.[26] The geometries of **2a** and **2b** were fully optimized without any symmetry constraints. The crystal structures were used as the starting geometries. The effect of the solvent was modeled by the CPCM dielectric model. Time dependent DFT (TD-DFT) calculations using the B3LYP functional were performed to obtain the UV–Vis and CD spectra of **2a**. The LANL2DZ basis set and effective core potential (ECP) for Cu(II) and 6-31G* basis set for other atoms were adopted in the TD-DFT calculations. The calculations of IR and VCD spectra of **2a** and **2b** were also carried out under B3LYP combined with the LANL2DZ basis set/ECP for Cu(II) and 6-31 G* for other atoms.

RESULTS AND DISCUSSION

Synthesis and Product Characterization

The macrocyclic imines and their copper coordination compounds were prepared using optically pure enantiomers of camphor. The copper coordination compounds **2a** and **2b** were characterized by elemental analyses, ESIMS, and NMR. Both the copper coordination compounds are resistant to air and moisture. The crystal structures of **2a** and **2b** have been determined by single crystal X-ray crystallography. Details of the crystal parameters, data collection, and refinements for **2a** and **2b** are summarized in Table 1. Selected bond lengths and angles for **2a** and **2b** are summarized in the supplementary material (Table S1).

Crystal Structure and Absolute Configuration

The geometric structures of the copper coordination compounds are similar to that of the nickel coordination compounds.[20] The chiral ligands chelate the copper ion via their four nitrogen donor atoms (Fig. S1). The CuN_4 core adopts a considerably distorted square-planar geometry toward tetrahedron. The camphor-sulfonyl groups are tilted with regard to the coordination plane, leading to a boat conformation

TABLE 1. Crystallographic data of compounds 2a and 2b

	2a·H_2O	**2b**·H_2O
Formula	$C_{24}H_{38}N_4O_4S_2Cu$	$C_{24}H_{38}N_4O_4S_2Cu$
Mr	592.26	592.26
Crystal system	Orthorhombic	Orthorhombic
Space group	$P2_1\,2_1\,2_1$	$P2_1\,2_1\,2_1$
a/Å	12.427(2)	12.386(2)
b/Å	12.895(2)	12.9123(16)
c/Å	17.865(3)	17.857(3)
$\alpha = \beta = \gamma$/°	90.00	90.00
V/Å^3	2862.7(9)	2586.0(8)
Z	4	4
T/K	291(2)	291(2)
Radiation, λ/Å	0.71073	0.71073
D_{calcd}/g cm^{-3}	1.374	1.377
μ/mm^{-1}	0.948	0.950
F(000)	1252	1252
Crystal size/mm^3	0.28 × 0.24 × 0.22	0.26 × 0.22 × 0.20
θrange/°	2.28–23.60	2.25–23.45
Reflections measured	15,388	15,332
Unique reflections	5570	5561
R_{int}	0.044	0.088
Reflections with $F^2 > 2\sigma(F^2)$	4827	4838
Number of parameters	347	347
Goodness-of-fit on F^2	1.055	1.074
R_1[a], wR_2[b] $[I > 2\sigma(I)]$	0.053, 0.112	0.060, 0.139
R_1, wR_2 (all data)	0.063, 0.115	0.065, 0.141
$\Delta\rho_{max}$, $\Delta\rho_{min}$/e Å^{-3}	0.24, −0.33	0.40, −0.44

[a] $R_1 = \Sigma(|Fo| - |Fc|)/\Sigma|Fo|$.
[b] $wR_2 = [\Sigma w(Fo^2 - Fc^2)^2/\Sigma w(Fo^2)^2]^{1/2}$.

of the central heterocyclic ring. The camphor imines have retained their *E* configuration after coordination to the metal. The enantiomeric structures are almost exact mirror images of each other (Fig. 1). According to the "skew-line system,"[15] the absolute configuration of copper coordination compound **2a** is Δ while **2b** is Λ.

UV–Visible Spectra, Circular Dichroism Spectra, and the Exciton Chirality Model[27–34]

The UV–vis and CD spectra of the free ligands and copper coordination compounds enantiomers are shown in Figure 2. The ligand **1a** shows an absorption band at $\lambda_{max} = 238$ nm with tailing to 300 nm. The copper complex **2a** shows three main peaks with the maxima around 203 ($\varepsilon = 1.7 \times 10^4$), 273 ($\varepsilon = 5.1 \times 10^3$), and 370 ($\varepsilon = 2.29 \times 10^3$) nm, respectively. In addition, a broad weak band with a maximum at about 627 ($\varepsilon = 0.2$–0.3×10^3) nm is detectable. The electronic spectra of **1b** and **2b** are essentially the same for both enantiomers. The CD spectrum of **1a** shows positive Cotton effects at 225 nm and negative Cotton effects at 255 nm, whereas the CD spectrum of **2a** exhibits positive Cotton effects at $\lambda_{max} = 249$ and 641 nm and negative Cotton effects at 213, 373, and 533 nm. The CD spectrum of **2b** is nearly a mirror image of that of **2a**. TD-DFT calculations based on the optimized structure of **2a** (selected optimized structural parameters are listed in Table S1) gave quite good simulation of UV–vis and CD spectra as shown in Figure 3. The experimental absorption bands could thus be assigned according to the calculations (Table S2 and Figs. S2 and S3).

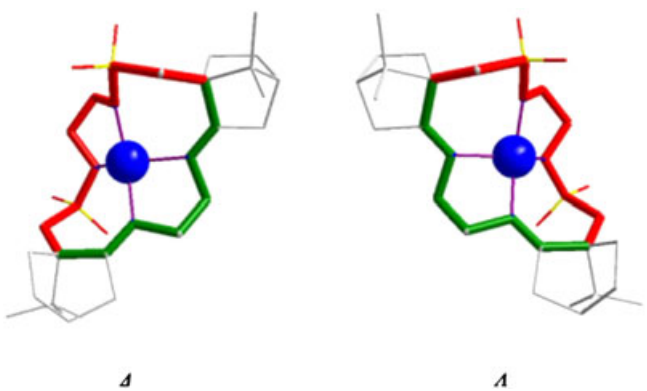

Fig. 1. The "mirror image" of X-ray crystal structures of the copper coordination compounds **2a** (left) and **2b** (right). [Color figure can be viewed in the online issue, which is available at wileyonlinelibrary.com.]

The band around 627 nm is associated with the electron transition from the weak σ-antibonding 3d orbital to the strongly σ-antibonding 3d orbital. The higher energy band at 370 and 273 nm corresponds to ligand–metal charge transfer, where the electronic transitions come from the imine ligand π orbitals and nonbonding nitrogen orbitals to the strongly antibonding 3d orbital.[29–31] The highest energy band around 203 nm can be assigned to the π–π* transition between imine ligands, which is evidenced by the similar absorption band observed for the free ligands (Fig. 2).

In the CD spectrum of **2a**, a positive–negative CD couplet within 651–556 nm was observed, which can be designated to the d–d transition. The split of the d–d transition in the CD spectrum is due to the asymmetric coordination environment of the Cu(II) ion. The CD signal of the d–d transition of **2a** is significantly higher compared with its nickel anologue.[20] The high CD intensity of the d–d transitions can be ascribed to metal–ligand (antibonding) orbital interactions that result in (out-of-phase) mixing of ligand π and/or σ orbitals with the d orbitals.[33,34] The band at 373 nm (negative Cotton effect) can be assigned as the ligand–metal charge transfer band at 370 nm. The intense negative band at 213 nm is primarily a π–π* transition.[30,31,33] As expected, compound **2b** displays Cotton effects of the opposite sign at the same wavelengths.

The absolute configuration of **2a** and **2b** can be determined from the CD spectra according to the exciton coupling model.[28,34] The CD spectrum of **2a** shows good bisignate Cotton effects in the d–d transition region with positive peaks at lower energy and negative peaks at higher energy, which is assigned as positive chirality. In contrast, compound **2b** shows opposite exciton couplet corresponding to negative chirality.[3,27,28] The CD exciton couplet in positive chirality is associated with the Δ configuration, whereas the CD exciton couplet in negative chirality is associated with the Λ configuration. Therefore, the absolute configuration of **2a** is Δ, whereas that of **2b** is Λ, which is in agreement with the absolute configuration determined by "skew-line system" via X-ray single crystal structure measurement. Our system thus represents a good example where the CD bisignate signal of d–d transition is observed and might be used to the determination of the absolute configuration for metal coordination compounds.

Infrared and Vibrational Circular Dichroism Spectra[35,36]

Figure 4 shows the IR and VCD spectra of copper coordination compounds enantiomers in $CDCl_3$ solutions in the mid-infrared region, whereas Figure 5 shows the IR and VCD

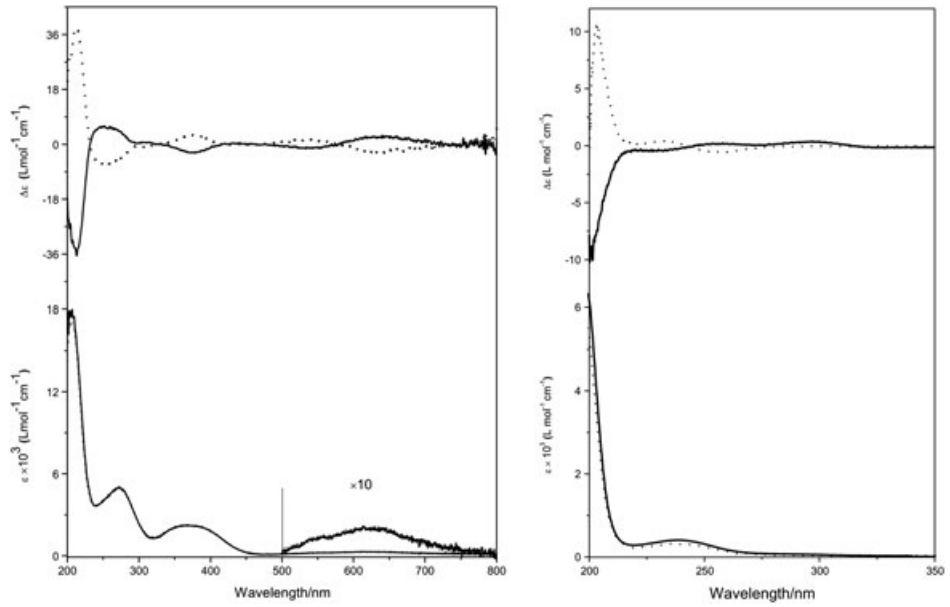

Fig. 2. Experimental ultraviolet–visible and circular dichroism spectra of copper(II) coordination compound **2a** (solid line) and **2b** (dot line) (left); and free ligands **1a** (solid line) and **1b** (dot line) in methanol solution (right).

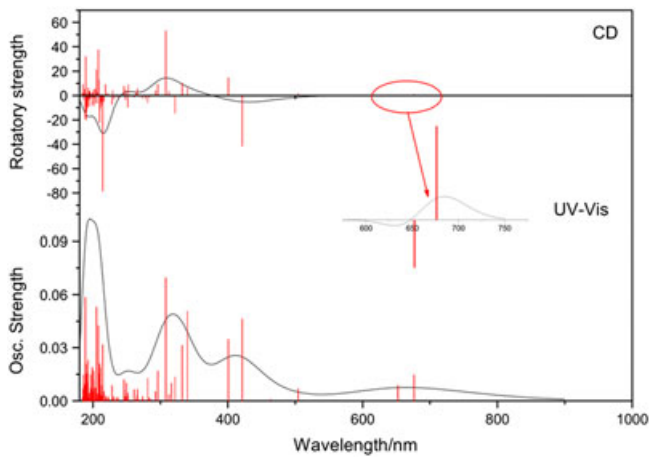

Fig. 3. Calculated ultraviolet–visible and circular dichroism spectra of coordination compound **2a** in methanol solution. [Color figure can be viewed in the online issue, which is available at wileyonlinelibrary.com.]

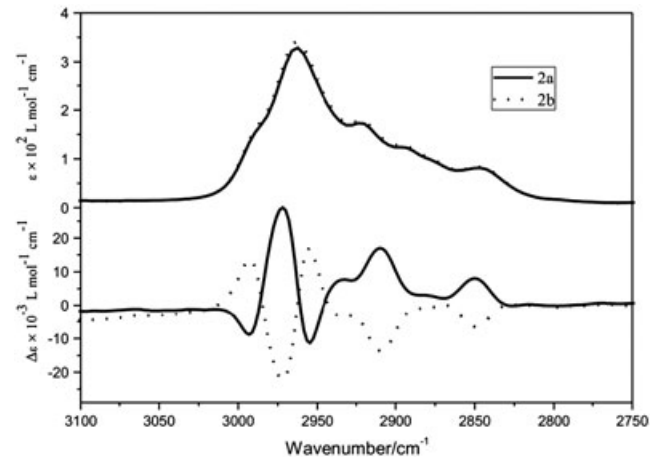

Fig. 5. Infrared (top) and vibrational circular dichroism (bottom) spectra in the C—H stretching region of copper coordination compounds **2a** and **2b** in $CDCl_3$ solution.

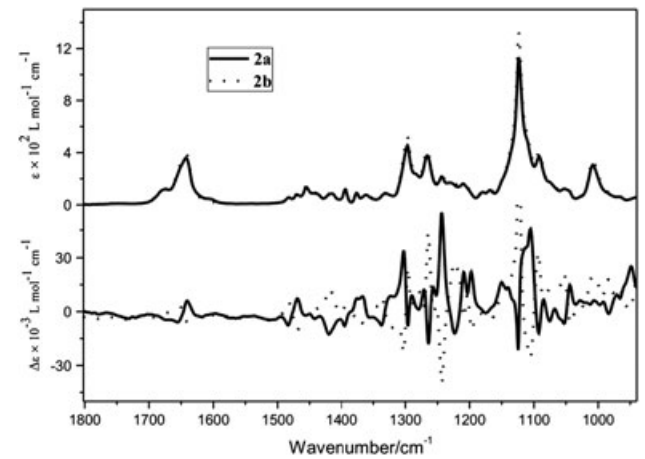

Fig. 4. Infrared (top) and vibrational circular dichroism (bottom) spectra in the mid-infrared region of copper coordination compounds **2a** and **2b** in $CDCl_3$ solution.

spectra of copper coordination compounds enantiomers in $CDCl_3$ solutions in the C-H stretching regions. As expected, the IR spectra of both enantiomers are almost the same, while the VCD spectra are nearly mirror images.

In the IR spectra, the strongest peaks in the mid-infrared region come from the imine double bond (1675 cm^{-1}) and sulfonamide (1297, 1266, and 1009 cm^{-1}) stretch vibrations, whereas the weaker peaks originate in the camphor skeleton and two ethyl-diamino group (1500–1300 cm^{-1}) stretch vibrations. Several overlapped peaks in the C-H stretching region can be assigned to C-H stretching of camphor and two ethyl-diamino groups.

To monitor the complexation process of ligand to copper(II) ion, the IR and VCD spectra of the imine ligands with the same concentration as their copper(II) coordination compound in $CDCl_3$ were obtained (Figs. S4 and S5). Comparison of IR and VCD spectra between free ligand **1a** and copper coordination

compound **2a** is shown in Figures 6 (mid-infrared region) and 7 (C-H stretching region).

As shown in Figure 6, principal bands of the coordination compound are blue shifted compared with the free ligand. The CN double bond stretching is visible as two absorption bands for **1a**: a weak peak around 1731 cm^{-1} and a stronger peak around 1677 cm^{-1}, which are shifted to 1675 and 1642 cm^{-1} for **2a**, respectively. The corresponding VCD signal of the ligand shows only one significant negative signal around 1677 cm^{-1} for **1a**, which turns to a bisignate signal (1655 cm^{-1} negative, 1640 cm^{-1} positive) for **2a**. The strong absorptions of the ligand at 1331 and 1149 cm^{-1} characteristic for the antisymmetric and symmetric stretching vibrations of sulfonamide group[37] exhibit as a strong bisignate signal (1332 cm^{-1} negative, 1322 cm^{-1} positive) and a strong positive peak at 1152 cm^{-1} in the VCD spectrum. The VCD spectrum is thus more sensitive to the complexation than absorption. Upon coordination to Cu(II), the two sulfonamide stretching bands are shifted to lower wavenumbers; the antisymmetric stretching vibrations show as two nearly equal intensity peaks at 1297 and 1266 cm^{-1}, whereas the symmetric stretching vibrations show as one higher intensity peak at 1123 cm^{-1} and the other lower intensity peak at 1092 cm^{-1} (on the basis of DFT calculation).

The IR and VCD spectra of the ligand **1a** and copper coordination compound **2a** in the C-H stretching region also exhibit some differences. The difference in IR spectra is quite small because of overlapping. A broad peak is present at 2956 for **1a** and 2961 cm^{-1} for **2a**, typical for C-H stretching of camphor molecule.[38–41]

In the VCD spectra, the antisymmetric stretching of the methyl (CH_3) groups is observed at 2988 cm^{-1} for **1a** and 2993 cm^{-1} for **2a** as a negative signal. The stretching of the CH_2-CH_2-C*H part of the ring[42,43] for **1a** appears as a triplet (+, −, +) at about 2970, 2952, and 2931 cm^{-1}, respectively, followed by a broad (+)-VCD feature at around 2908 cm^{-1} assigned to the CH_2 C-H stretching of the ethylamine group. For **2a**, these peaks are shifted to 2972, 2955, 2909, and 2849 cm^{-1}, respectively.

The simulated and experimental IR and VCD spectra in the mid-IR and C-H stretching regions are compared in Figures 8 and S6, respectively. Selected experimental and calculated IR peaks with their assignments are listed in Table 2. Both the IR and VCD spectra are reproduced reasonably well by the present set of parameters, although there are some discrepancies. In the mid-IR region (Fig. 8), the strongest absorptions of the free ligand are contributed from the CN stretching (1757 and 1749 cm^{-1}) and the antisymmetric

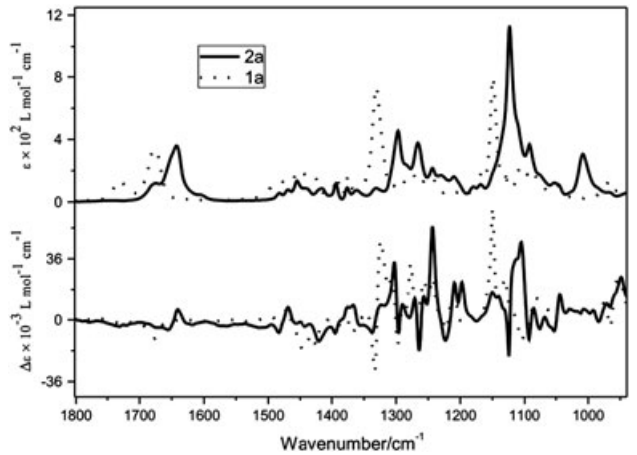

Fig. 6. Infrared (top) and vibrational circular dichroism (bottom) spectra in the mid-infrared region of copper coordination compound **2a** and free ligand **1a** in $CDCl_3$ solution.

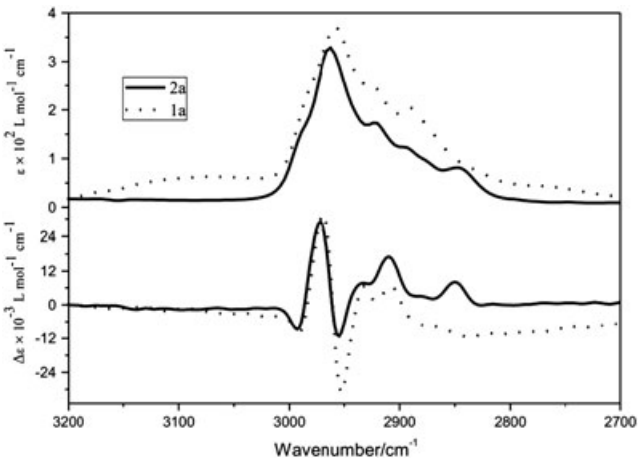

Fig. 7. Infrared (top) and vibrational circular dichroism (bottom) spectra in the C—H stretching region of copper coordination compound **2a** and free ligand **1a** in $CDCl_3$ solution.

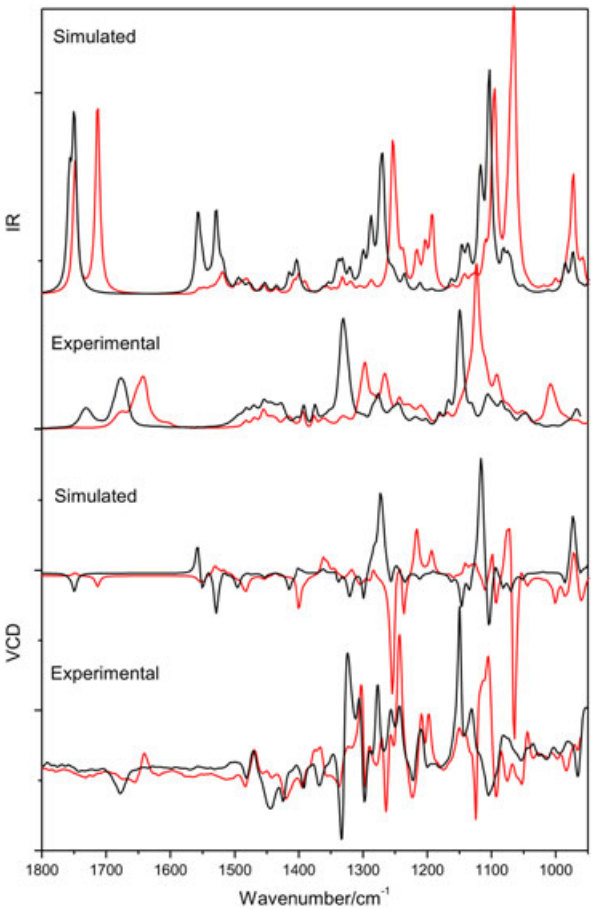

Fig. 8. Infrared and vibrational circular dichroism spectra of **1a** (black line) and **2a** (red line) in the mid-infrared region measured in d-chloroform and the B3LYP calculations. [Color figure can be viewed in the online issue, which is available at wileyonlinelibrary.com.]

TABLE 2. Comparison of the selected experimental infrared spectral features for 2a to the calculated transitions (see Fig. 8)

Exp.	Calc.	Assignment
1675	1748	C=N stretching
1642	1713	C=N stretching
1482	1556	C—H deformation of camphor skeleton
1470	1526	
1455	1490	
1415	1454	
1393	1437	
1376	1408	C—H deformation of NCH_2CH_2N
1362	1400, 1390	
1297	1253	Antisymmetric stretching of —SO_2—
1123	1094	Symmetric stretching of —SO_2—
1092	1065	
1009	973	S—N stretching

(1273 and 1269 cm^{-1}) and symmetric stretching vibrations (1118 and 1103 cm^{-1}) of the sulfonamide group. When coordinated with Cu(II), these absorption bands are all shifted to short wavenumbers, which is in accordance with experimental results. The intense bands at 1529 and 1557 cm^{-1} of the free ligand could be assigned to the N—H deformation according to the calculation. These bands were somewhat weaker in the measured spectra, probably because of an influence of the intramolecular hydrogen bonding between SO_2N—H and C=N. Also in Figure 7, very weak (~3100 cm^{-1}) N—H stretching vibrations are apparent both in IR and VCD spectra in the C-H stretching region. However, attempts to optimize the structure of the free ligand with intramolecular hydrogen bonding were not successful.

The N—H deformation vibrations disappeared in both the simulated and experimental IR spectrum of copper(II) coordination compound, indicating that the two hydrogen atoms were fully replaced by a copper(II) ion. In the simulated VCD spectra, the C=N stretching of the free ligand exhibits a weak negative Cotton effect, whereas the antisymmetric and symmetric stretching vibrations of the sulfonamide group show sharp bisignate signal. All these predicted features are in good agreement with the measurements. In the C—H stretching region (Fig. S6), the frequency agreement between the simulation and the experiment is not as good as that in the mid-IR region. However, the C—H stretching of —CH_2CH_2— of the ethylamine group can be clearly identified in the lowest wavenumber region. In the free ligand, this band is close to the CH stretching of camphor backbone. When coordinated to copper(II) ion, the frequency shifts (to ~2849 cm^{-1} in experiment). The computation of the C—H stretching region within the harmonic approximation may not be accurate because of possible anharmonic effects including Fermi resonances.[38] However, in our case, main IR and VCD intensity features appeared to be reproduced reasonably well. The IR and VCD experimental and calculated intensities of free ligand and complex are quite similar, which reflects the rigid structure of the macrocyclic ligand. The coordination process influences mainly the stretching motion of groups (C=N, —SO_2NH—) around the copper(II) ion center, more visible in the lower wavenumber (<2000 cm^{-1}) region.

There is a general belief that VCD is less predictable for open-shell systems.[21,22] However, the calculation of VCD spectra of Λ- and Δ-[Ru(acac)$_3$] has been successfully performed by Sato *et al.*[44,45] Our results also show that the magnetic field perturbation theory for VCD calculation can be extended to open-shell systems.

The *anisotropy ratio* (*g-factor*), also called *dissymmetry factor*, is CD signal normalized by the corresponding isotropic absorption. We can thus compare experiment and theory using

$$g = \Delta\varepsilon/\varepsilon = 4\mathrm{R}/\mathrm{D}$$

where $\Delta\varepsilon$ and ε are the experimental molar CD and molar absorption coefficient and R and D are the rotational and dipole strengths of the corresponding calculated transition.[46,47]

The VCD *g*-factor is usually in the range of 10^{-4} to 10^{-5} if there are no enhancement effects. In a study of the $[Co(en)_3]^{3+}$ transition metal complex, the intensity increased about 10 times, most probably due to a presence of low-lying excited electronic states.[47] Table 3 lists the *g*-factors of the selected transitions measured in this study. The observed VCD signals of imine double bonds stretch vibrations (1675 and 1642 cm^{-1}) are much stronger compared with those obtained by the DFT simulation. On the other hand, the calculated *g*-factor of the antisymmetrical stretch vibrations of sulfonamide is bigger than the measured one. We attribute the other discrepancies between the theory and experiment at least partially to the same effect as for the cobalt coordination compound,[46] that is, to an interference of electronic states,[16,17] although some can be caused by a limited basis set used for the calculation.[48] The *g*-factors of the symmetric stretch vibrations of sulfonamide are not compared because the VCD signal to noise ratio is small because of strong IR absorption. The experimental and calculated *g*-factors of S—N stretching are in a very good agreement.

CONCLUSIONS

We have synthesized open-shell systems of copper coordination compounds enantiomers derived from both camphor enantiomers as a model for CD complex studies both in the UV–vis and IR region. Their absolute configurations were

TABLE 3. Selected vibrational circular dichroism bands of the experimental and calculated frequencies and anisotropy *g*-factor for 2a (see Fig. 8)

	Exp.		Calc.	
	Frequency	Anisotropy	Frequency	Anisotropy
C=N stretching	1675	3.84×10^{-5}	1748	2.73×10^{-6}
C=N stretching	1642	1.66×10^{-5}	1713	6.58×10^{-6}
Antisymmetric stretching of —SO_2—	1297	1.13×10^{-5}	1253	9.96×10^{-5}
S—N stretching	1009	2.05×10^{-5}	973	1.95×10^{-5}

determined by X-ray crystallography and by comparison of the CD and VCD experimental spectra to the calculation. The TD-DFT calculations reproduced the UV–vis and CD spectra quite well, which enabled a reliable assignment of the CD and absorption bands and also the determination of the absolute configuration. The configurations could be determined from the CD bisignate signal of the d–d transition also according to the simplified exciton model.

The VCD spectroscopy both in the mid-infrared and C—H stretching regions provided the same configuration as CD. Most spectral peaks could be assigned to local vibrational motions in the coordination compound and the free ligand. IR frequency shifts of the imine and sulphonamide group vibrations in the free ligands and coordination complexes accompanied the complex formation. These could be faithfully modeled. Similar spectral changes were exhibited for VCD, although the agreement between the simulated and experimental shapes was worse than for IR. A slight discrepancy between the calculated and observed *g*-factors was partially explained by the electronic VCD enhancement. Thus, the spectroscopic methods if combined with the computations can be used to characterize the structure and coordination properties of chiral ligands and their copper coordination compounds. The presented results also manifest that in particular the VCD spectroscopy is an excellent chiroptical technique to monitor the coordination process. For chiral ligand, the spectroscopy can probe the process of chiral recognition. For future applications, an accuracy increase of the computations and experiment is desirable.

ACKNOWLEDGMENTS

The authors would like to thank Prof. Marie Urbanová and Dr. Ondřej Julínek of the Institute of Chemical Technology, Prague, for their help on VCD measurement. The authors would also like to thank the China Scholarship Council and the Ministry of Education of the People's Republic of China for the financial support.

LITERATURE CITED

1. Berova N, Nakanishi K, Woody RW, editors. Circular dichroism, principles and applications, 2nd ed. New York: Wiley; 2000.
2. Urbanová M, Malo P. Circular dichroism spectroscopy. In: Schalley C, editor. Analytical methods in supramolecular chemistry. Weinheim: Wiley-VCH; 2007, p 265–303.
3. Berova N, Bari LD, Pescitelli G. Application of electronic circular dichroism in configurational and conformational analysis of organic compounds. Chem Soc Rev 2007;36:914–931.
4. Stephens PJ, Devlin FJ, Pan JJ. The determination of the absolute configurations of chiral molecules using vibrational circular dichroism (VCD) spectroscopy. Chirality 2008;20:643–663.
5. Sadlej J, Dobrowolski JC, Rode JE. VCD spectroscopy as a novel probe for chirality transfer in molecular interactions. Chem Soc Rev 2010;39:1478–1488.
6. Urbanová M, Setnika V, Devlin FJ, Stephens PJ. Determination of molecular structure in solution using vibrational circular dichroism spectroscopy: the supramolecular tetramer of *S*-2,2′-dimethyl-biphenyl-6, 6′-dicarboxylic acid. J Am Chem Soc 2005;127:6700–6711.
7. Pessoa JC, Correia I, Goncalves G, Tomza I. Circular dichroism in coordination compounds. J Argent Chem Soc 2009;97:151–165.
8. Yang GC, Xu YJ, Hou JB, Zhang H, Zhao YF. Determination of the absolute configurations of the pentacoordinate chiral phosphorus compounds in solution using vibrational circular dichroism spectroscopy and density functional theory. Chem Eur J 2010;16:2518–2527.
9. Julínek O, Urbanová M, Lindner W. Enantioselective complexation of carbamoylated quinine and quinidine with N-blocked amino acids: vibrational and electronic circular dichroism study. Anal Bioanal Chem 2009;393:303–312.
10. Montigny FD, Guy L, Pilet G, Vanthuyne N, Roussel C, Lombardi R, Freedman TB, Nafie LA, Crassous J. Subtle chirality in oxo- and sulfidorhenium(V) complexes. Chem Commun 2009;32:4841–4843.
11. Abbate S, Lebon F, Gangemi R, Longhi G, Spizzichino S, Ruzziconi R. Electronic and vibrational circular dichroism spectra of chiral 4-X-[2.2] paracyclophanes with X containing fluorine atoms. J Phys Chem A 2009;113:14851–14859.
12. Gottarelli G, Lena S, Masiero S, Pieraccini S, Spada GP. The use of circular dichroism spectroscopy for studying the chiral molecular self-assembly: an overview. Chirality 2008;20:471–485.
13. Amouri H, Gruselle M. Chirality in transition metal chemistry: molecules, supramolecular assemblies and materials. Chichester: Wiley-VCH; 2008.
14. Crassous J. Chiral transfer in coordination complexes: towards molecular materials. Chem Soc Rev 2009;38:830-845.
15. Knof U, Zelewsky A. Predetermined chirality at metal centers. Angew Chem Int Ed 1999;38:302-322.
16. He YN, Cao XL, Nafie LA, Freedman TB. Ab initio VCD calculation of a transition-metal containing molecule and a new intensity enhancement mechanism for VCD. J Am Chem Soc 2001;123:11320–11321.
17. Nafie LA. Theory of vibrational circular dichroism and infrared absorption: extension to molecules with low-lying excited electronic states. J Phys Chem A 2004;108:7222–7231.
18. Sato H, Shirotani D, Yamanari K, Kaizaki S. Vibrational circular dichroism of Δ-SAPR-8-tetrakis [(+)-heptafluorobutyrylcamphorato]lanthanide(III) complexes with an encapsulated alkali metal ion. Inorg Chem 2010;49:356–358.
19. Sato H, Taniguchi T, Nakahashi A, Monde K, Yamagishi A. Effects of central metal ions on vibrational circular dichroism spectra of tris-(β-diketonato)metal(III) complexes. Inorg Chem 2007;46:6755-6766.
20. Wu T, Li CH, Li YZ, Zhang ZG, You XZ. Synthesis, structure and chiroptical study of chiral macrocyclic imine nickel (II) coordination compounds derived from camphor. Dalton Trans 2010;39:3227-3232.
21. Cheeseman JR, Frisch MJ, Devlin FJ, Stephens PJ. Ab initio calculation of atomic axial tensors and vibrational rotational strengths using density functional theory. Chem Phys Lett 1996;252:211–220.
22. Stephens PJ. Theory of vibrational circular dichroism. J Phys Chem 1985;89:748–752.
23. SAINT-Plus, version 6.02. Madison, WI: Bruker Analytical X-ray System; 1999.
24. Sheldrick GM. SADABS. An empirical absorption correction program. Madison, WI: Bruker Analytical X-ray Systems; 1996.
25. Sheldrick GM. SHELXTL-97. Göttingen, Germany: Universität of Göttingen; 1997.
26. Frisch MJ, Trucks GW, Schlegel HB, Scuseria GE, Robb MA, Cheeseman JR, Scalmani G, Barone V, Mennucci B, Petersson GA, Nakatsuji H, Caricato M, Li X, Hratchian HP, Izmaylov AF, Bloino J, Zheng G, Sonnenberg JL, Hada M, Ehara M, Toyota K, Fukuda R, Hasegawa J, Ishida M, Nakajima T, Honda Y, Kitao O, Nakai H, Vreven T, Montgomery JA, Jr., Peralta JE, Ogliaro F, Bearpark M, Heyd JJ, Brothers E, Kudin KN, Staroverov VN, Kobayashi R, Normand J, Raghavachari K, Rendell A, Burant JC, Iyengar SS, Tomasi J, Cossi M, Rega N, Millam JM, Klene M, Knox JE, Cross JB, Bakken V, Adamo C, Jaramillo J, Gomperts R, Stratmann RE, Yazyev O, Austin AJ, Cammi R, Pomelli C, Ochterski JW, Martin RL, Morokuma K, Zakrzewski VG, Voth GA, Salvador P, Dannenberg JJ, Dapprich S, Daniels AD, Farkas O, Foresman JB, Ortiz JV, Cioslowski J, Fox DJ. Gaussian 09, Revision A.02. Wallingford CT: Gaussian, Inc.; 2009.
27. Telfer SG, McLean TM, Waterland MR. Exciton coupling in coordination compounds. Dalton Trans 2011;40:3097–3108.
28. Harada N, Nakanishi K. The exciton chirality method and its application to configurational and conformational studies of natural products. Acc Chem Res 1972;5:257-263.
29. Ziegler M, Zelewsky A. Charge-transfer excited state properties of chiral transition metal coordination compounds studied by chiroptical spectroscopy. Coord Chem Rev 1998;177:257–300.
30. Wojtczak A, Szlyk E, Jaskolski M, Larsen E. An optically active nickel (II) Schiff base coordination compound N, *N′*-(1*R*,2*R*)-(−)-1, 2-cyclehexylenebis(salicylideneiminato)nickel(II). Acta Chem Scand 1997;51:274–278.
31. Pasini A, Gullotti M, Ugo R. Optically active complexes of Schiff bases. Part 4. An analysis of the circular-dichroism spectra of some complexes of different co-ordination numbers with quadridentate Schiff bases of optically active diamines. JCS Dalton Trans 1977;4:3346–356.

32. Fan J, Autschbach J, Ziegler T. Electronic structure and circular dichroism of tris(bipyridyl) metal complexes within density functional theory. Inorg Chem 2010;49:1355–1362.
33. Wang F, Zhang H, Li L, Hao HQ, Wang XY, Chen JG. Synthesis and characterization of chiral nickel (II) Schiff base complexes and their CD spectra–absolute configuration correlations. Tetrahedron Asymmetry 2006;17:2059–2063.
34. Bosnich B. The application of exciton theory to the determination of the absolute configurations of inorganic complexes. Acc Chem Res 1969;2:266–273.
35. Nicu VP, Autschbach J, Baerends EJ. Enhancement of IR and VCD intensities due to charge transfer. Phys Chem Chem Phys 2009;11:1526–1538.
36. Freedman TB, Cao XL, Young DA, Nafie LA. Density functional theory calculations of vibrational circular dichroism in transition metal complexes: identification of solution conformations and mode of chloride ion association for (+)-tris(ethylenediaminato)cobalt(III). J Phys Chem A 2002;106:3560–3565.
37. Nakamoto K. Infrared spectra of inorganic and coordination compounds. New York: Wiley; 1978.
38. Gangemi F, Gangemi R, Longhi G, Abbate S. Calculations of overtone NIR and NIR-VCD spectra in the local mode approximation: camphor and camphorquinone. Vib Spectrosc 2009;50:257–267.
39. Abbate S, Burgi LF, Gangemi F, Gangemi R, Lebon F, Longhi G, Pultz VM, Lightner DA. Comparative analysis of IR and vibrational circular dichroism spectra for a series of camphor-related molecules, J Phys Chem A 2009;113:11390–11405.
40. Longhi G, Abbate S, Gangemi R, Giorgio E, Rosini C. Fenchone, camphor, 2-methylenefenchone and 2-methylenecamphor: a vibrational circular dichroism study. J Phys Chem A 2006;110:4958–4968.
41. Longhi G, Gangemi R, Lebon F, Castiglioni E, Abbate S, Pultz VM, Lightner DA. A comparative study of overtone CH-stretching vibrational circular dichroism spectra of fenchone and camphor. J Phys Chem A 2004;108:5338–5352.
42. Laux L, Pultz V, Abbate S, Havel HA, Overend J, Moscowitz A. Inherently dissymmetric chromophores and vibrational circular dichroism. The CH2-CH2-C*H fragment. J Am Chem Soc 1982;104:4276–4278.
43. Gangemi R, Longhi G, Lebon F, Abbate S, Laux L. Vibrational excitons in CH-stretching fundamental and overtone vibrational circular dichroism spectra. Monatshefte für Chemie 2005;136:325–345.
44. Sato H, Mori Y, Fukuda Y, Yamagishi A. Syntheses and vibrational circular dichroism spectra of the complete series of [Ru((−)- or (+)-tfac)$_n$(acac)$_{3-n}$] (n = 0 ~ 3, tfac = 3-trifluoroacetylcamphorato and acac = acetylacetonato). Inorg Chem 2009;48:4354–4361.
45. Sato H, Unoa H, Nakano H. Identification of geometrical isomers using vibrational circular dichroism spectroscopy: a series of mixed-ligand complexes of diamagnetic Co(III) ions. Dalton Trans 2011;40:1332–1337.
46. Johannessen C, Thulstrup PW. Vibrational circular dichroism spectroscopy of a spin-triplet bis-(biuretato) cobaltate(III) coordination compound with low-lying electronic transitions. Dalton Trans 2007;36:1028–1033.
47. Bormett RW, Smith GD, Asher SA, Barrick D, Kurtz DM. Vibrational circular dichroism measurements of ligand vibrations in haem and non-haem metalloenzymes . Faraday Discuss 1994;99:327–339.
48. Bouř P, McCann J, Wieser H. Measurement and calculation of absolute rotational strengths for camphor, α-pinene, and borneol. J Phys Chem A 1998;102:102–110.